J. KOSAE Vol. 24, No. E 2 (2008) pp. 92 ~ 101
Journal of Korean Society for Atmospheric Environment

Predictability Experiments of Fog and Visibility in Local Airports over Korea using the WRF Model

Cheol-Han Bang*, Ji-Woo Lee[1] and Song-You Hong[2]
Global Environment Research Center, National Institute of Environmental Research, Incheon, Korea
[1]*Republic of Korea Air Force, 73th Weather Group, Daejeon, Korea*
[2]*Department of Atmospheric Sciences, Global Environment Laboratory, Yonsei University, Seoul, Korea*

(Received 25 November 2008, accepted 18 December 2008)

Abstract

The objective of this study is to evaluate and improve the capability of the Weather Research and Forecasting (WRF) model in simulating fog and visibility in local airports over Korea. The WRF model system is statistically evaluated for the 48-fog cases over Korea from 2003 to 2006. Based on the 4-yr evaluations, attempts are made to improve the simulation skill of fog and visibility over Korea by revising the statistical coefficients in the visibility algorithms of the WRF model. A comparison of four existing visibility algorithms in the WRF model shows that uncertainties in the visibility algorithms include additional degree of freedom in accuracy of numerical fog forecasts over Korea. A revised statistical algorithm using a linear-regression between the observed visibility and simulated hydrometeors and humidity near the surface exhibits overall improvement in the visibility forecasts.

Key words : Visibility, Fog, Weather Research and Forecasting (WRF), Statistical method

1. INTRODUCTION

Generally, fog is a visibility-restricting suspension of tiny water droplets or ice crystals near the surface. Fog presents a serious hazard in airports of intense traffic, and its prediction is essential for public safety and has a high economic value (Croft, 2003; Leigh, 1995). Aviation meteorological fog, in particular, is defined as an obscuration phenomenon with the prevailing visibility less than 1 mile (National Weather Service, 2004). Thus, it is ascertained that accurate prediction of fog and visibility is critically important in aviation meteorology. In predicting fog and deriving visibility using the numerical weather prediction (NWP) model outputs, its accuracy depends upon not only predicted meteorological variables associated with fog, but also the statistical algorithm deriving the visibility from the variables.

The NWP models for visibility calculation usually have used the relationship between the observed visibility and simulated liquid water content (LWC) or temperature (T), relative humidity (RH). In real atmospheric conditions, visibility is related to droplet number and water mass in a given volume of air

* Corresponding author.
Tel : +82-32-560-7913, E-mail : chbang@me.go.kr

(Gultepe *et al.*, 2001). The increase of droplet number concentrations (N_d) in warm-fog conditions ($T > 0°C$) for a fixed LWC results in the decrease of visibility. Also, increasing LWC results in decreasing visibility that is currently represented with visibility-LWC relationships in most of the existing NWP models (e.g., Stoelinga and Warner, 1999, SW99 hereinafter). A key point for the success of this approach is that the fog phenomenon is associated with the comprehensive physical processes such as cloud microphysics, radiative transfer, horizontal and vertical diffusions in the planetary boundary layer (PBL) that are forced by the prevailing synoptic background as well as mesoscale disturbances (Chun *et al.*, 1999; Croft *et al.*, 1997).

The local airports over the Korean Peninsula have often been affected by fog. Most of the airports are located near coastal areas of the peninsula, thus their aviation forecasts being largely influenced by sea fog; the Tsushima Current originating from the Kuroshio, supplies heat to the east sea and south sea throughout the year, while the west sea is characterized by shallow water under strong tidal currents, due to the fact that it influences fog event over all coastal area around the Korean Peninsula (Cho *et al.*, 2000). It was also reported that the public airline industry loses billions of dollars annually due to airport shutdowns by fog in Korea (Sinkevich *et al.*, 2001). Despite the accumulated understanding about the characteristics of fog over Korea by analyzing the observational data (e.g., Ahn *et al.*, 2002; Seo *et al.*, 2001; Heo, 1998), and devising the forecast algorithms using the statistical methods (e.g., Eom and Kim, 2002), accurate prediction of the fog's occurrence, duration, and intensity are still a challenging task to the Korean scientists. One of the possible reasons is geographical uniqueness of the Korean peninsula (Lee *et al.*, 2003; Kim *et al.*, 2000).

The purpose of the present study is to evaluate the prediction skill of fog and visibility using the Weather and Research Forecast (WRF) model (Skamarock *et al.*, 2005), focusing on the regional airports over Korea. The 48 fog events from 2003 to 2006 are selected to evaluate the existing visibility algorithms in the WRF model and to devise a revised method through a statistical adjustment.

2. CASE DESCRIPTION

In this study, a total of 48 fog cases are selected for 4 years from 2003 to 2006 (Table 1), in order to analyze the characteristics of fog by season and region under the conditions with Korea's state-of-the-art airport environments when the dam constructions around airports such as Incheon International Airport or inland airport were completed. Rainy days and Asian-dust days are excluded in the indicated cases to remove severe visibility accompanied by other atmospheric phenomena. These cases were selected in individual sections as the fog days that occurred during the identical period. The region of South Korea is classified into three sections, namely section I (Westerly coast region), section II (South-easterly coast region) and section III (Inland region) (Fig. 1a); and four airports which represent the climatic characteristics in each region are chosen in this study (Fig. 1b).

Radiation fog or advection fog occurs frequently in the westerly coastal region (section I). Radiation fog is one of the most common types of fog, which is caused by the radiation cooling of the ground. Favorable conditions for its formation constitute clear sky, little or no wind, and a small temperature-dew point spread. It is primarily a nighttime occurrence, but it often begins to form in the late afternoon and may not dissipate until well after sunrise. On the other hand, advection fog is influenced by shallow water under strong tidal currents. The temperature of the west sea is lower than 16°C. Incheon, Osan, Gunsan, and Mokpo are selected to investigate the predictability of fog in section I. The mean annual fog days and duration for 4 cities are 26.2 and 4.0 hours, respectively.

South-easterly coastal region (section II) experiences mainly advection fog. Advection fog can form when warm, moist air blows over cool land or water. Unlike radiation fog, advection fog moves to an area, sometimes as a thick bank of fog that engulfs the area. Yeosu, Gimhae, Pohang, and Gangneung are

Table 1. A description of 48 selected fog cases from 2003 to 2006. The regional airports are depicted in Fig. 1.

Year	Section	Spring	Summer	Autumn	Winter
2003	I	12 UTC 8 Mar. ~ 12 UTC 9 Mar.	12 UTC 3 Aug. ~ 12 UTC 4 Aug.	12 UTC 27 Nov. ~ 12 UTC 28 Nov.	12 UTC 8 Feb. ~ 12 UTC 9 Feb.
	II	12 UTC 9 Apr. ~ 12 UTC 10 Apr.	12 UTC 29 Jun. ~ 12 UTC 30 Jun.	12 UTC 1 Oct. ~ 12 UTC 2 Oct.	12 UTC 8 Feb. ~ 12 UTC 9 Feb.
	III	12 UTC 11 Apr. ~ 12 UTC 12 Apr.	12 UTC 1 Jun. ~ 12 UTC 2 Jun.	12 UTC 17 Nov. ~ 12 UTC 18 Nov.	12 UTC 7 Feb. ~ 12 UTC 8 Feb.
2004	I	12 UTC 14 Mar. ~ 12 UTC 15 Mar.	12 UTC 22 Jul. ~ 12 UTC 23 Jul.	12 UTC 7 Oct. ~ 12 UTC 8 Oct.	12 UTC 6 Jan. ~ 12 UTC 7 Jan.
	II	12 UTC 8 Mar. ~ 12 UTC 9 Mar.	12 UTC 9 Jul. ~ 12 UTC 10 Jul.	12 UTC 4 Nov. ~ 12 UTC 5 Nov.	12 UTC 28 Nov. ~ 12 UTC 29 Nov.
	III	12 UTC 8 May ~ 12 UTC 9 May	12 UTC 5 Aug. ~ 12 UTC 6 Aug.	12 UTC 9 Nov. ~ 12 UTC 10 Nov.	12 UTC 1 Feb. ~ 12 UTC 2 Feb.
2005	I	12 UTC 15 Mar. ~ 12 UTC 16 Mar.	12 UTC 29 Jun. ~ 12 UTC 30 Jun.	12 UTC 26 Oct. ~ 12 UTC 27 Oct.	12 UTC 25 Jan. ~ 12 UTC 26 Jan.
	II	12 UTC 22 Mar. ~ 12 UTC 23 Mar.	12 UTC 23 Jun. ~ 12 UTC 24 Jun.	12 UTC 5 Oct. ~ 12 UTC 6 Oct.	12 UTC 26 Jan. ~ 12 UTC 27 Jan.
	III	12 UTC 29 May ~ 12 UTC 30 May	12 UTC 22 Jul. ~ 12 UTC 23 Jul.	12 UTC 1 Oct. ~ 12 UTC 2 Oct.	12 UTC 25 Jan. ~ 12 UTC 26 Jan.
2006	I	12 UTC 5 Mar. ~ 12 UTC 6 Mar.	12 UTC 21 Jul. ~ 12 UTC 22 Jul.	12 UTC 15 Oct. ~ 12 UTC 16 Oct.	12 UTC 14 Jan. ~ 12 UTC 15 Jan.
	II	12 UTC 16 Mar. ~ 12 UTC 17 Mar.	12 UTC 27 Jun. ~ 12 UTC 28 Jun.	12 UTC 15 Oct. ~ 12 UTC 16 Oct.	12 UTC 22 Dec. ~ 12 UTC 23 Dec.
	III	12 UTC 5 Mar. ~ 12 UTC 6 Mar.	12 UTC 27 Jun. ~ 12 UTC 28 Jun.	12 UTC 15 Oct. ~ 12 UTC 16 Oct.	12 UTC 14 Jan. ~ 12 UTC 15 Jan.

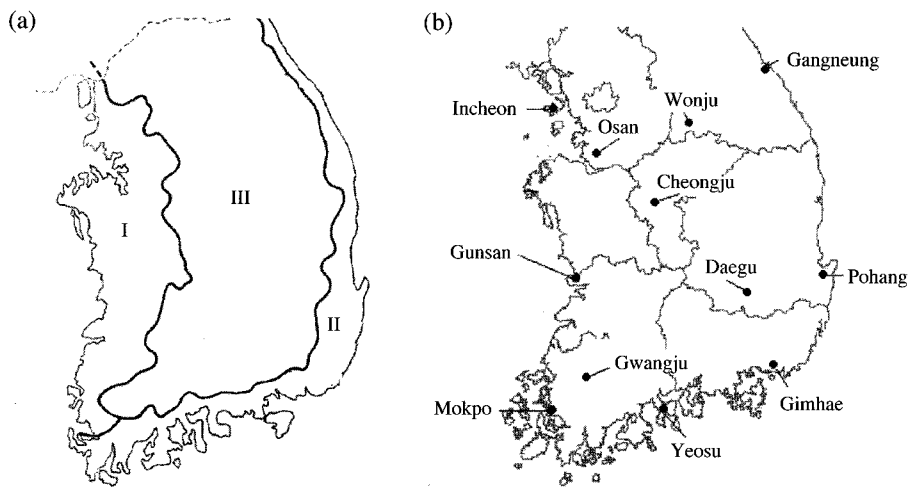

Fig. 1. (a) Classification of the sections based on the characteristics of fog in Korea, and (b) the location of airports in Korea. Each section has four airports.

selected for section II. The mean annual number of fog days is very low to 18.5 days and seasonal ratio is highest in summer. The average duration of fog occurrence is very long in spring and summer to 4.3

hours. The fog dispersal appears during the whole period of time. Because the Tsushima Current affects the temperature of the south and east seas, most of the south and east sea temperatures are warmer than 17~18°C, respectively, except in some coastal regions. In consideration of the conditions stated above, the fog occurrence is concentrated mainly in summer, accompanied by advection fog.

As for an inland region (section III), Gwangju, Wonju, Cheongju, and Daegu where the radiation fog frequently occurs are selected. In this region, fog mostly occurs by the radiation cooling of the boundary layer. The mean annual number of fog days is 45.2 and the mean fog duration is 4.3 hours. The fog occurs mainly by the nocturnal radiation cooling and is dispersed by the surface heating and turbulence.

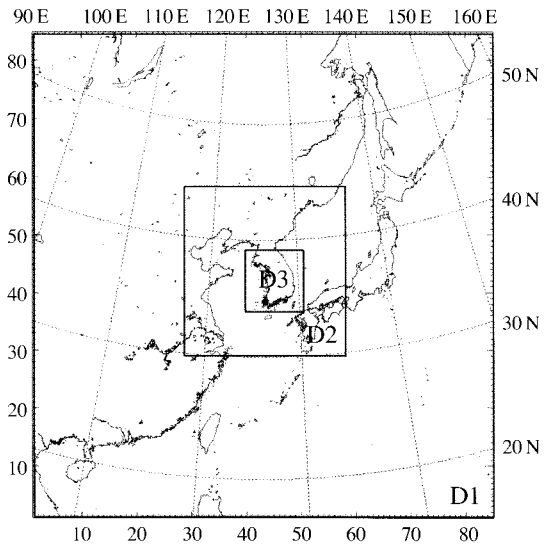

Fig. 2. The WRF model domains for a 54 km (D1), 18 km (D2), and 6 km (D3).

3. MODEL DESCRIPTION

The Advanced Research WRF (ARW; Skamarock *et al.*, 2005) is a community model suitable for both research and forecasting. This model has a good potential for simulating mesoscale phenomena. The model used in this study is the WRF version 2.1.2, which was released in January 2006. The physics packages other than the microphysics include the Kain (2004) cumulus parameterization scheme, the 5-layer thermal diffusion model, the Yonsei University planetary boundary layer (YSUPBL) (Hong *et al.*, 2006), WRF Single-Moment 6-class (WSM6) scheme (Hong and Lim, 2006; Hong *et al.*, 2004), and Rapid Radiative Transfer Model (RRTM) longwave radiation schemes (Mlawer *et al.*, 1997).

The model configuration consisted of a nested domain configuration defined in the Lambert conformal space. A 6-km grid model covering South Korea except for Jeju Island (Domain 3, 85 × 85), was surrounded by a 18-km grid model (Domain 2, 85 × 85), which in turn was surrounded by a 54-km grid model (Domain 1, 85 × 85) by a two-way interaction (Fig. 2). All grid systems had 40 vertical layers and the model top was located at 50 mb. No cumulus parameterization was used at the 6-km grid model. Only the 6-km outputs will be used for visibility evaluations here, based on the study of Bang (2007).

Initial and boundary conditions are preprocessed through a separate package called the WRF standard Initialization. This was done using the global analysis and prediction system that is routinely produced at the Center for Environmental Prediction (NCEP) Global Data Assimilation System (GDAS). This data with 1° × 1° degree grid is available every 6 hours. A 24-hr simulation forced by the GDAS data is conducted for 48 events in Table 1 to apply the visibility algorithm. The output interval is 1 hour.

4. VISIBILITY ALGORITHMS IN THE WRF MODEL

In version 2.2.1 of the WRF model, there are four visibility algorithms as described below. A revised formula devised in this study is given at the end of this section.

4.1 Steolinga and Warner method (SW99)

Stoelinga and Warner (1999) Method calculates the visibility using the predicted cloud water (cw), cloud ice (ci), rain (rw), and snow (sn), which can be

Table 2. Relationships between the mass concentration (C, gm^{-3}) and the extinction coefficient (β, km^{-1}) in the Steolinga and Warner (1999) scheme.

Hydrometeor	Relationship
Cloud liquid water, fog	$\beta_{cw}=144.7\,C^{0.88}$
Rain	$\beta_{rw}=1.1\,C^{0.75}$
Cloud ice	$\beta_{ci}=163.9\,C^{1.00}$
Snow	$\beta_{sn}=10.4\,C^{0.78}$

expressed by,

$$x_{vis}(km)=\frac{-\ln(0.02)}{\beta} \quad (1)$$

where $\beta=\beta_{cw}+\beta_{rw}+\beta_{ci}+\beta_{sn}$. The extinction coefficientis β (km^{-1}) a function of number concentration for each type of hydrometeor, as given in Table 2.

4.2 Rapid Update Cycle (RUC) method

In the RUC visibility algorithm that was adopted from the RUC model, surface visibility is based on the RH (%), as given by,

$$VIS(km)=60\exp\left[-2.5\times\frac{(RH-15)}{80}\right] \quad (2)$$

4.3 Forecast Systems Laboratory (FSL) method

This algorithm is specifically devoted to products relating directly to flight or other hazardous weather. The surface visibility algorithm was also developed by National Oceanic & Atmospheric Administration (NOAA)/Forecast Systems Laboratory (FSL) (Doran *et al.*, 1999), in which surface visibility is based on the state of the RH and dew point depression (T−Td) (°C) where:

$$VIS(mile)=6000\times\frac{T-Td}{RH^{1.75}} \quad (3)$$

4.4 A combined visibility method (CVIS)

This algorithm is a combined approach of the SW99 and FSL methods. This method simultaneously calculates the two methods, and then selects the lower visibility, and can be written by,

$$VIS(mile)=\min(SW99, FSL) \quad (4)$$

4.5 A revised algorithm developed in this study (RVIS)

The RVIS algorithm is a combined method of the two SW99 and FSL algorithms, as expressed by,

$$VIS(mile)=\alpha\times SW99+\delta\times(T-Td)/RH^{1.75} \quad (5)$$

where the coefficients, α and δ, are responsible for the intraseasonal variation of visibility. These coefficients are derived from a statistical evaluation between the observed visibility and the computed visibility from the SW99 and FSL methods. A regression method with a harmonic analysis is applied to provide the coefficients from the simulated 48 fog events. The harmonic analysis consists of representing the fluctuations or variations in a time series as having arisen from the adding together of a series of sine and cosine functions. These trigonometric functions are "harmonic" in the sense that they are chosen to have frequencies exhibiting integer multiples of the "fundamental" frequency determined by the sample size of the data series. In this case, the time series is conformable to the Julian date (JD), which is a continuous count of days and fractions elapsed since the same initial epoch. Refer to Bang (2007) for further details.

As shown in Fig. 3, this revised algorithm (RVIS) accounts for the seasonal and intraseasonal variations of the relationship between the computed visibility and meteorological variables. This method follows the CVIS method in terms of a combined approach of the two existing algorithms, but adds the seasonal and intraseasonal variation to the prescribed algorithms, together with the regional characteristics. The derived coefficients generally follow the seasonal dependency of fog frequencies, as demonstrated in Ahn *et al.* (2002).

5. RESULTS AND DISCUSSION

The root mean square errors (RMSE; km) and bias (km) of the predicted visibility are shown in Tables 3 and 4, respectively. The SW99 algorithm shows the worst performance, and the RUC, FSL, and CVIS in that order. The performance of SW99

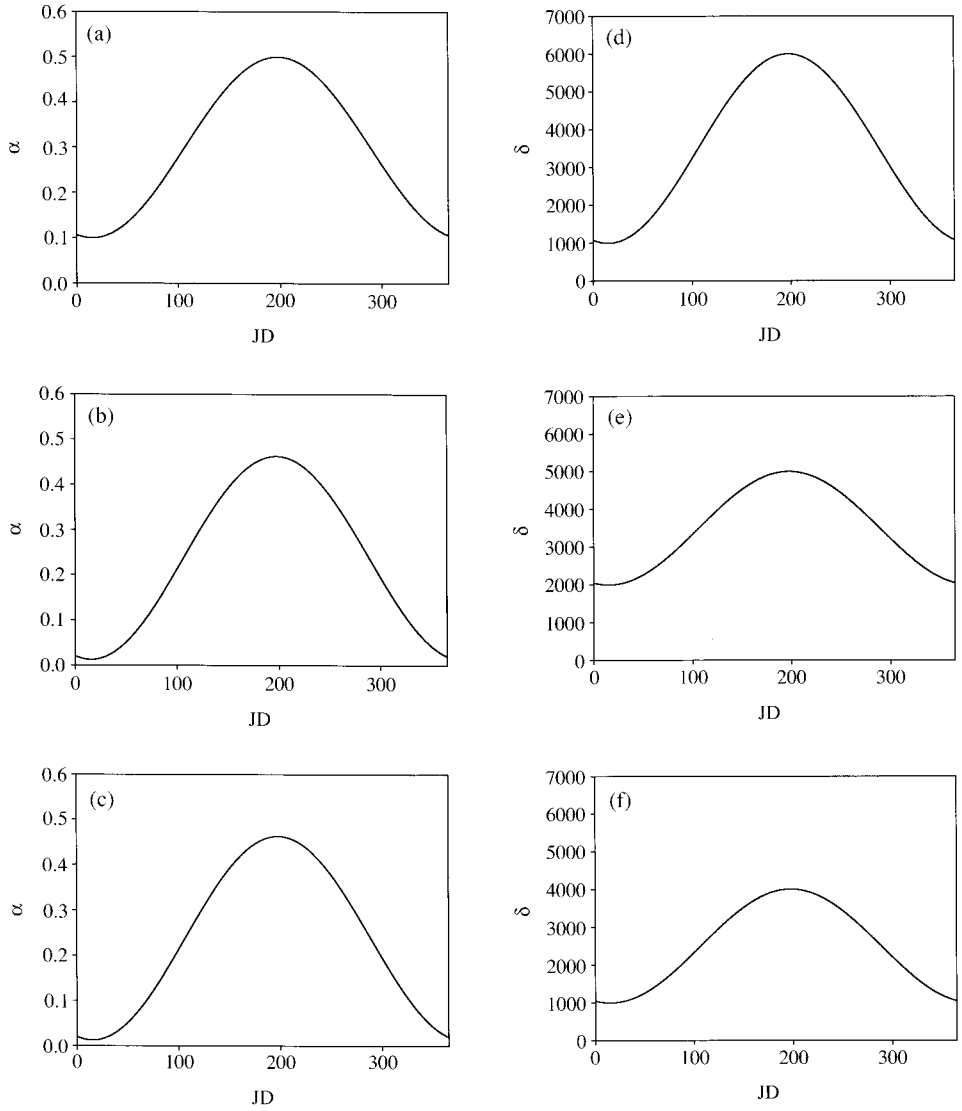

Fig. 3. Seasonal and regional distribution of the coefficients in the visibility algorithm (RVIS). The left and right panels represent the temporal dependency of α and δ, respectively, in Eq. (5), with respect to the Julian data (JD). The upper, middle, and lower panels stand for sections, I, II, and III, respectively.

shows the worst value, because the extinction coefficient was derived and tuned from the observation of the relatively low-pressure regions in the United States, which if applied to the Korean regions, brings on easy dissipation as the extinction coefficient to be applied is larger than its actual value. The RUC method and FSL methods utilize the relative humidity information, which perform better than the SW99 over Korea, but are not significantly. The CVIS method turns out to be the best one among the existing four algorithms, but still tends to underestimate the visibility.

It is noted that the existing 4 algorithms exhibit the maximum errors in autumn irrespective of the

Table 3. Root-Mean-Square-Error (RMSE, km) of the simulated visibility for the 48 fog events.

Methods	Section	Spring	Summer	Autumn	Winter	Average
SW99	I	6.67	5.71	7.49	6.56	5.58
	II	4.82	5.28	5.60	3.87	
	III	4.38	5.25	5.90	5.50	
RUC	I	6.16	4.72	6.85	5.58	5.01
	II	3.74	4.48	5.20	3.33	
	III	4.58	4.70	5.63	5.09	
FSL	I	5.68	4.96	6.37	5.04	4.94
	II	4.14	4.40	5.02	3.60	
	III	4.70	4.69	5.63	5.01	
CVIS	I	5.63	4.86	6.43	5.01	4.86
	II	3.95	4.22	4.98	3.42	
	III	4.70	4.83	5.47	4.80	
RVIS	I	4.45	4.74	5.30	3.54	4.24
	II	3.94	4.05	4.34	2.96	
	III	4.67	3.89	4.61	4.45	

Table 4. Same as in Table 3, but the bias (km).

Methods	Section	Spring	Summer	Autumn	Winter	Average
SW99	I	−4.64	−3.58	−6.72	−4.85	−4.03
	II	−3.65	−3.90	−4.53	−2.43	
	III	−1.98	−4.21	−4.54	−3.47	
RUC	I	−3.79	−1.39	−1.39	−3.42	−2.54
	II	−1.50	−2.72	−3.34	−1.46	
	III	−1.20	−3.18	−4.18	−2.94	
FSL	I	−3.22	−0.16	−0.16	−3.10	−2.21
	II	−1.52	−2.08	−3.14	−2.02	
	III	−1.34	−2.80	−4.13	−2.99	
CVIS	I	−2.91	0.11	0.11	−2.88	−1.95
	II	−1.47	−1.74	−2.90	−1.79	
	III	−1.07	−2.35	−3.98	−2.66	
RVIS	I	−1.01	−2.13	−4.08	1.18	−0.74
	II	−0.38	−1.81	−1.47	−0.08	
	III	0.21	1.87	−2.72	1.44	

regions, with the minimum errors in section II regardless of the seasons, whereas the revised method designed in this study does not show a distinct systematic behavior. It implies that the proposed method properly takes into account the temporal and regional dependency of the visibility characteristics.

It is not surprising to see that the RVIS method outperforms the existing algorithms since this new one is formulated based on the statistical coefficients for the selected 48 cases. A further objective of the RVIS method is designed for four fog events that occurred over the Incheon Airport in 2007. As seen in Fig. 4, the RVIS method outperforms the CVSI method for all the four events. Both algorithms tend to overestimate the visibility, but the overall biases are smaller in the RVIS than in the CVIS algorithm. The proposed method effectively reduces the nighttime bias, as compared to the CVIS approach, but the performance in the daytime is mixed. For example, the dissipation of fog in the case of 3 is

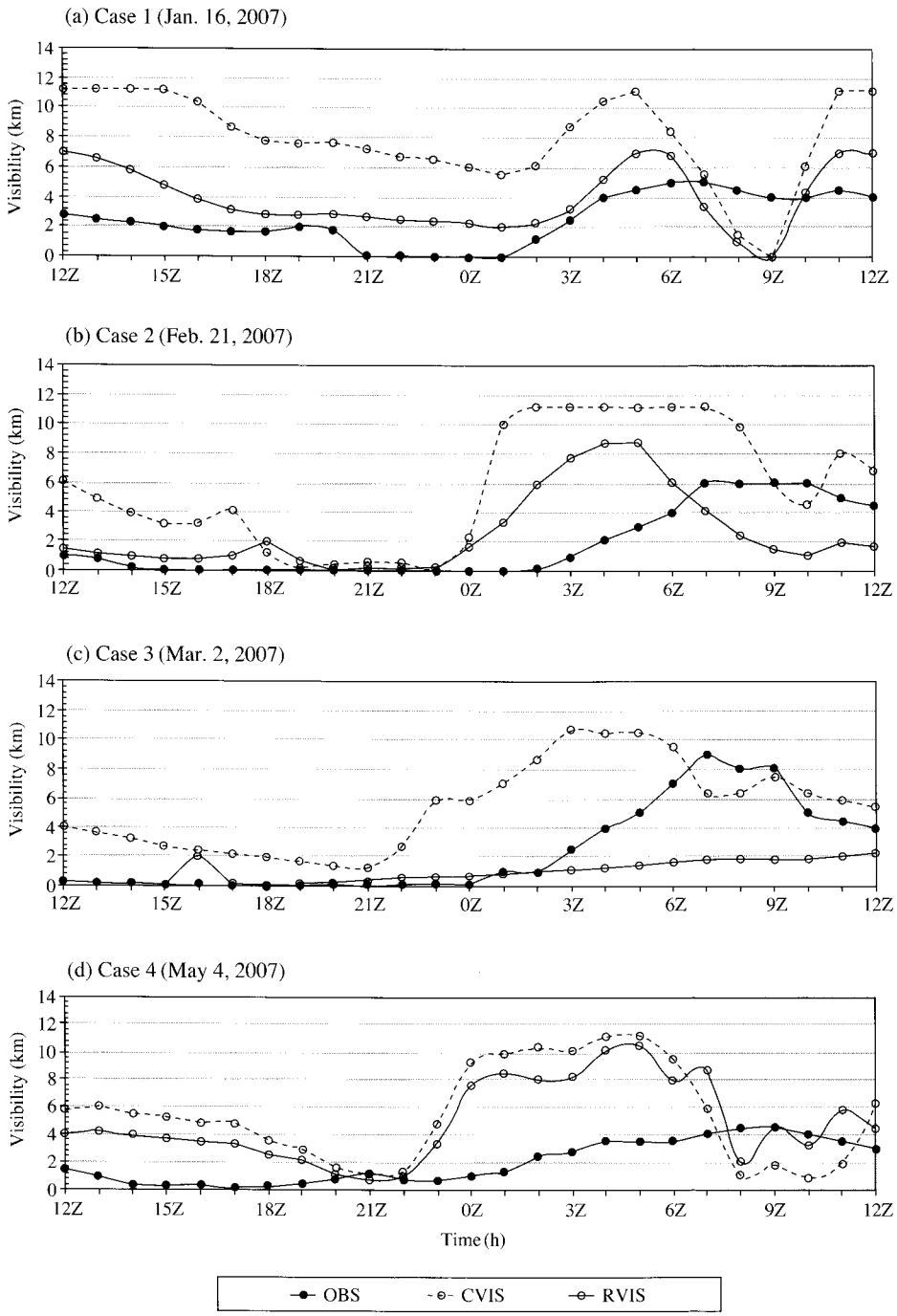

Fig. 4. Time series of visibility for four cases of fog events in Inchon airports in 2007, obtained from observations (solid lines with closed circles), and the WRF outputs with the CVIS (dashed lines with open circles), and RVIS (solid lines with open circles) algorithms.

not properly simulated.

6. CONCLUDING REMARKS

The results obtained in this study indicate that the visibility prediction is sensitive to the predicted mass concentrations of hydrometeors and moisture amount. This study also suggests that the accuracy of the visibility forecasts in local airports over Korea can be improved by applying a simple statistical adjustment to the existing visibility algorithm. It is ascertain because the coefficients in the visibility algorithm in the WRF are derived from the observational characteristics of fog over US, which should be properly modified to reflect the dynamical characteristics and geographical uniqueness associated with fog over Korea.

Our proposed method is merely another empirical formula for a given model setup, considering the seasonal and regional dependency of fog over Korea. Overall improvement of the model performance for short-range forecasts would guarantee the improved visibility forecasts, but the corresponding model-output-statistics correction should be followed. It is of no doubt that the observational characteristics of fog over Korea must be identified.

ACKNOWLEDGEMENTS

The authors sincerely thank the Korea Meteorological Administration (KMA) and the Republic of Korea Air Force (ROKAF) staffs for providing the satellite images and observed visibility and fog data. This research was supported by ROFAF through the project of "The Construction of Very Short-Term and Local Weather Forecasting System for the Support of Air Operation".

REFERENCES

Ahn, J.-B., J.-C. Nam, J.-W. Seo, and H.-J. Lee (2002) A study on the characteristics of fog over the Korean Peninsula, Atmos. Res., 12(1), 616-618.

Bang, C.-H. (2007) A numerical simulation study of fog and visibility in local airports over the Korean Peninsula using the WRF model, Master thesis, Yonsei University, Seoul, Korea, pp. 84.

Cho, Y.-K., M.-O. Kim, and B.-C. Kim (2000) Sea fog around the Korean Peninsula, J. Appl. Meteor., 39, 2473-2479.

Chun, Y.-S., K.-O. Boo, J.-Y. Kim, S.-W. Kim, H.-M. Cho, and S. Hong (1999) Analysis of the radiation fog at the Kimpo International Airport in autumn, J. of Atmos. Res., 16(1), 30-43.

Croft, P.J. (2003) Fog. In Encyclopedia of Atmospheric Sciences (J.R. Holton Ed), Academic Press, pp. 777-792.

Croft, P.J., R.L. Pfost, J.M. Medlin, and A.J. Johnson (1997) Fog forecasting for the southern region: a conceptual model approach, Wea. Forecasting, 12, 545-556.

Doran, J.A., P.J. Roohr, D.J. Beberwyk, G.R. Brooks, G. A. Gayno, R.T. Williams, J.M. Lewis, and R.J. Lefevre (1999) The MM5 at the Air Force Weather Agency-New products to support military operations, The 8th Conference on Aviation, Range, and Aerospace Meteorology, Dallas, Texas, 10-15 January.

Eom, K.-C. and N.-W. Kim (2002) Development of fog prediction model using statistical process, Atmosphere Res., 12(1), 292-294.

Gultepe, I., G.A. Isaac, and K. Strawbridge (2001) Variability of cloud microphysical and optical parameters obtained from aircraft and satellite remote sensing during RACE, Int. J. Climatol., 21, 507-525.

Heo, I.-H. (1998) The spatial distribution and characteristics of fog in Korea, The Korean Association of Geographic and Environmental Education, 6, 71-86.

Hong, S.-Y. and J.-O. Jade Lint (2006) The WRF Single-Moment 6-Class Microphysics Scheme (WSM6), J. Korean Meteor. Soc., 42(2), 129-151.

Hong, S.-Y., J. Dudhia, and S.-H. Chen (2004) A revised approach to ice-microphysical processes for the bulk parameterization of cloud and precipitation, Mon. Wea. Rev., 132, 103-120.

Hong, S.-Y., Y. Noh, and J. Dudhia (2006) A new vertical diffusion package with an explicit treatment of entrainment processes, Mon. Wea. Rev., 134, 2318-2341.

Kain, J.S. (2004) The Kain-Fritsch convective parameterization: an update, J. Appl. Meteor., 43, 170-181.

Kim, J., S.N. Oh, Y. Chun, J.C. Choi, and H.K. Min (2000) Fog forecast for the Kimpo International Airport of Korea. Preprints Conference on Aviation, Range, and Aerospace Meteorology, Amer. Met. Society, Orlando FL, pp. 219-222.

Lee, H.-Y., Y.-H. Lee, and D.-E. Chang (2003) A numerical experiment of fog in Yongdong Province and the northeast air current, Atmosphere Res., 13(3), 108-109.

Leigh, R.J. (1995) Economic benefits of Terminal Aerodrome Forecasts (TAFs) for Sydney Airport, Australia, Meteor. Appl., 2, 239-247.

Mlawer, E.J., S.J. Taubman, P.D. Brown, M.J. Iacono, and S.A. Clough (1997) Radiative transfer for inhomogeneous atmospheres: RRTM, a validated correlated-k model for the longwave, J. Geophys. Res., 102(D14), 16663-16682.

National Weather Service, Aviation Services Branch (2004) Terminal Aerodrome Forecasts. NWS Instruction 10-813. U.S. Department of Commerce, National Oceanic & Atmospheric Administration, National Weather Service Headquarter, Silver Spring, MD.

Seo, J.-W., J.-C. Nam, and Y.-C. Kim (2001) Analysis of the characteristics of fog occurrence around Youngjong-Do, Atmosphere Res., 11(1), 300-303.

Sinkevich, A., J.-Y. Kim, A.-S. Suh, and H.-S. Chung (2001) Losses in the Korean economy due to lack of routine cloud seeding, J. Korean Meteor. Soc., 37, 283-294.

Skamarock, W.C., J.B. Klemp, J. Dudhia, D.O. Gill, D.M. Barker, W. Wang, and J.G. Powers (2005) A Description of the Advanced Research WRF Version 2. NCAR technical note, NCAR/TN-468+STR, pp. 88.

Stoelinga, M.T. and T.T. Warner (1999) Nonhydrostatic, mesobeta-scale model simulations of cloud ceiling and visibility for an East Coast winter precipitation event, J. Appl. Meteor., 38, 385-404.